

# BiPS, a Photocleavable, Isotopically Coded, Fluorescent Cross-linker for Structural Proteomics\*

Evgeniy V. Petrotchenko‡, Kunhong Xiao§¶, Jennifer Cable‡, Yiwen Chen‡, Nikolay V. Dokholyan‡, and Christoph H. Borchers‡||

Cross-linking combined with mass spectrometry is an emerging approach for studying protein structure and protein-protein interactions. However, unambiguous mass spectrometric identification of cross-linked peptides derived from proteolytically digested cross-linked proteins is still challenging. Here we describe the use of a novel cross-linker, bimeane bithiopropionic acid *N*-succinimidyl ester (BiPS), that overcomes many of the challenges associated with other cross-linking reagents. BiPS is distinguished from other cross-linkers by a unique combination of properties: it is photocleavable, fluorescent, homobifunctional, amine-reactive, and isotopically coded. As demonstrated with a model protein complex, RNase S, the fluorescent moiety of BiPS allows for sensitive and specific monitoring of the different cross-linking steps, including detection and isolation of cross-linked proteins by gel electrophoresis, determination of in-gel digestion completion, and fluorescence-based separation of cross-linked peptides by HPLC. The isotopic coding of BiPS results in characteristic ion signal “doublets” in mass spectra, thereby permitting ready detection of cross-linker-containing peptides. Under MALDI-MS conditions, partial photocleavage of the cross-linker occurs, releasing the cross-linked peptides. This allows differentiation between dead-end, intra-, and interpeptide cross-links based on losses of specific mass fragments. It also allows the use of the isotope doublets as mass spectrometric “signatures.” A software program was developed that permits automatic cross-link identification and assignment of the cross-link type. Furthermore photocleavage of BiPS assists in cross-link identification by allowing separate tandem mass spectrometry sequencing of each peptide comprising the original cross-link. By combining the use of BiPS with MS, we have provided the first direct evidence for the docking site of a phosphorylated G-protein-coupled receptor C terminus on the multifunctional adaptor protein  $\beta$ -arrestin, clearly demonstrating the broad potential and application of this novel cross-linker

in structural and cellular biology. *Molecular & Cellular Proteomics* 8:273–286, 2009.

Numerous cellular processes involve stable or transient protein-protein interactions. Deciphering protein interaction networks and the organization of protein complexes, such as those involved in G-protein-coupled receptor and  $\beta$ -arrestin signaling, is a major focus of modern proteomics and cellular biology. An important emerging technology for the structural analysis of proteins and protein complexes involves cross-linking combined with advanced mass spectrometric techniques (1–4). This approach typically involves proteolysis of complexed proteins followed by mass spectrometric identification of the cross-linked peptides (also called “cross-links”) (5).

Unfortunately, experiments combining cross-linking with mass spectrometry involve many technical challenges. For example, the combinatorial nature of protein cross-links creates an intrinsic problem of identification when assayed by mass alone. Additionally insufficient fragmentation of cross-linked peptides during MS/MS sequencing often results in mass spectra that are difficult to interpret. The relatively low number of cross-links compared with non-cross-linker-containing peptides produced during proteolysis of the protein complex presents another analytical challenge.

Several recent developments have resolved some of these issues. Mass spectrometers capable of determining molecular weight with high mass accuracy, such as FTICR-MS instruments, reduce the number of potential cross-links that can be assigned to a specific mass (1, 6). Also the specific mass spectrometric “signature” provided by isotopically coded cross-linkers (7) and isotope labeling of cross-links during proteolysis (8) has been a crucial development for straightforward MS detection of cross-links. We recently reported an isotopically coded, chemically cleavable cross-linker that allows discrimination between cross-link types (dead end, intrapeptide, or interpeptide) and facilitates subsequent MS/MS sequencing of the individual peptides that constitute an interpeptide cross-link (9). We have also reported a specific photocleavage of fluorescent monobromo-

From the ‡Department of Biochemistry and Biophysics, University of North Carolina, Chapel Hill, North Carolina 27599 and §Department of Medicine, Duke University, Durham, North Carolina 27710

Received, June 13, 2008, and in revised form, September 23, 2008

Published, MCP Papers in Press, October 6, 2008, DOI 10.1074/mcp.M800265-MCP200

bimane (MBB)<sup>1</sup>-labeled cysteine residues that occurs under MALDI conditions (10).

Based on this observation, we designed a cross-linker called BiPS (bimane bithiopropionic acid *N*-succinimidyl ester) that is structurally similar to MBB-modified cysteine and can therefore be photocleaved under MALDI conditions (see Fig. 1A). Eight deuterium atoms were incorporated into the structure of H<sub>8</sub>-BiPS (D<sub>8</sub>-BiPS) to assist in the detection of both the cross-links and the peptides obtained after photocleavage when a 1:1 mixture of H<sub>8</sub>-BiPS and D<sub>8</sub>-BiPS is used. H<sub>8</sub>-BiPS/D<sub>8</sub>-BiPS mixtures thus allow complementary detection of the cross-links by fluorescence and by MS. Laser-induced photocleavage of the cross-linker facilitates cross-link identification and cross-link type assignment by a combination of accurate mass and MS/MS sequencing of each individual peptide. These characteristics make this novel cross-linker a powerful tool for studying protein structure and protein-protein interactions. Here we report a proof-of-principle study of the interaction of G-protein-coupled receptors (GPCRs) and  $\beta$ -arrestins using our novel cross-linker. GPCRs, also referred to as "seven membrane-spanning receptors," constitute the largest known family of cell surface receptors. These proteins are common targets of modern drug therapy because they mediate a diverse group of intercellular signaling events (11). The dynamic sensitivity of GPCR function and signaling is due in large part to their regulation by the G-protein-coupled receptor kinase/ $\beta$ -arrestin system. Upon agonist activation, G-protein-coupled receptor kinase-mediated phosphorylation of the C terminus of the receptor initiates binding of the multifunctional adaptor and transducer proteins, the  $\beta$ -arrestins, to the receptor. This interaction leads to the desensitization of G-protein-mediated signaling, internalization of the receptor, and activation of a growing list of  $\beta$ -arrestin-dependent signaling cascades and cellular processes. However, little is known about the structural basis of this interaction. Although a complete elucidation of the structural basis must await resolution of the atomic structure of the receptor- $\beta$ -arrestin complex, our structural proteomics methodology (combining MS with the novel BiPS cross-linker) has provided new direct structural information on the interaction between GPCR and  $\beta$ -arrestin.

## EXPERIMENTAL PROCEDURES

### Synthesis of BiPS/D<sub>8</sub>-BiPS

All reagents were purchased from Sigma-Aldrich unless otherwise noted. BiPS cross-linker was synthesized by mixing mercaptopropionic acid and dibromobimane followed by activation with *N*-hydroxysuccinimide. Mercaptopropionic and *d*<sub>4</sub>-mercaptopropionic acids were synthesized as described elsewhere (12). Briefly bromopropi-

onic acid (0.65 mmol) or *d*<sub>4</sub>-bromopropionic acid (C/D/N Isotopes Inc.) was mixed with 0.65 mmol of thiourea and 200  $\mu$ l of water or D<sub>2</sub>O, respectively. The mixture was heated for 2 h at 99 °C, and 100  $\mu$ l of 40% (w/w) NaOH or NaOD (Isotec) was then added and incubated for 1 h at 99 °C in a Thermomixer (Eppendorf). Each preparation was adjusted to pH ~8 with HCl, and 0.1 mmol of dibromobimane (Calbiochem) was added. The solution was mixed until completely dissolved and kept at room temperature for 1 h. The pH was adjusted to ~8 by addition of NaOH (for H<sub>8</sub>-BiPS) or NaOD (for D<sub>8</sub>-BiPS). Bimane bithiopropionic acid was precipitated by addition of HCl, filtered, washed with 1 mM HCl, and lyophilized. Equal amounts of H<sub>8</sub>- and D<sub>8</sub>-dicarboxylic acids were mixed, dissolved in DMSO, and activated with *N*-hydroxysuccinimide and dicyclohexylcarbodiimide overnight at room temperature. The reaction mixture was then filtered, and BiPS was precipitated by the addition of water, washed with water, and lyophilized. BiPS and its deuterated derivative were characterized by nano-ESI (QSTAR, Applied Biosystems, Framingham, MA) under the experimental conditions and parameter settings described elsewhere (13).

### Protein Cross-linking Procedure

**Cross-linker Solution**—A 1:1 mixture of H<sub>8</sub>-BiPS:D<sub>8</sub>-BiPS was used for all cross-linking reactions. Cross-linkers were stored as 10 mM stock solution in DMSO at -20 °C and were added directly to a solution of the protein in PBS to give a final concentration as described below.

**Cross-linking of RNase S**—RNase S (1 mg/ml in PBS, pH 8.0) was cross-linked with 0.5 mM BiPS for 30 min at 25 °C. The reaction was quenched by adding 50 mM ammonium bicarbonate, and proteins were separated by SDS-PAGE. Protein bands containing cross-linker were visualized using a UV illuminator with a 362-nm excitation filter. The fluorescent band, corresponding to cross-linked RNase S, was excised and in-gel digested with porcine trypsin (sequencing grade, Promega) according to the protocol described previously (14, 15), separated by HPLC, and analyzed by MALDI-MS as described below.

**Cross-linking of  $\beta$ -Arrestins and V<sub>2</sub>Rpp**—The synthesis of phosphopeptide V<sub>2</sub>Rpp and the corresponding non-phosphorylated peptide, V<sub>2</sub>Rnp, have been described previously (16). The peptide sequence is ARGRTPPSLGPQDESCTTASSSLAKDTSS (phosphorylated residues are underlined). The procedures for purification of rat  $\beta$ -arrestin 1 was subcloned into a pGEX4T1 vector and overexpressed in *Escherichia coli* strain BL21(DE3)pLysS. Clarified cell lysate was loaded onto a glutathione-Sepharose column, and  $\beta$ -arrestin 1 was cleaved from the affinity-bound GST- $\beta$ -arrestin 1 by digestion with thrombin. The cleaved  $\beta$ -arrestin 1 was further purified on a 5-ml HiTrap Mono Q column followed by gel filtration on a Superdex 75 column. For the cross-linking reaction, two samples were run in parallel: one with V<sub>2</sub>Rpp and the other with V<sub>2</sub>Rnp, both in a 1:1 ligand:protein ratio. One picomole of  $\beta$ -arrestin 1 in PBS buffer, pH 8.0, was incubated with V<sub>2</sub>Rpp or V<sub>2</sub>Rnp and 0.25 mM cross-linker for 30 min at 25 °C. Unreacted cross-linker was quenched by incubation with 100 mM ammonium bicarbonate for ~20 min after which the sample was separated by SDS-PAGE. Finally the corresponding protein band was in-gel digested overnight at 25 °C with trypsin (1:10 molar ratio of trypsin to  $\beta$ -arrestin) and analyzed by MALDI-MS as described below.

Rat  $\beta$ -arrestin 2 was overexpressed in *E. coli* as C-terminally His-tagged protein and was purified using nickel-nitrilotriacetic acid-Sepharose followed by gel filtration on Superdex 75. Two cross-linking reactions were run in parallel: with and without V<sub>2</sub>Rpp. One nanomole of  $\beta$ -arrestin 2 in PBS buffer, pH 8.0, was incubated with 0.25 mM cross-linker for 30 min at 25 °C with or without V<sub>2</sub>Rpp.

<sup>1</sup> The abbreviations used are: MBB, monobromobimane; ICC-CLASS, isotopically coded cleavable cross-linking analysis software suite; GPCR, G-protein-coupled receptor; EGSS, ethylene glycol bis(sulfosuccinimidylsuccinate); V<sub>2</sub>R, vasopressin type II receptor; BiPS, bimane bithiopropionic acid *N*-succinimidyl ester.

Unreacted cross-linker was quenched by incubation with 100 mM ammonium bicarbonate for ~20 min, digested with trypsin (1:10 molar ratio) overnight at 37 °C, separated by HPLC, and analyzed by MALDI-MS as described below.

**HPLC Separation of Cross-linked Peptides**—Tryptic peptides were separated and collected (1-ml fractions) by reversed phase HPLC with fluorescence detection using a 60-min linear gradient of 5–65% acetonitrile in 0.1% TFA at 1 ml/min on an HP1100 (Agilent) LC instrument equipped with a Vydac 218TP54 (C<sub>18</sub>, 5  $\mu$ m, 250  $\times$  4.6-mm) column (The Nest Group, Inc., Southborough, MA). Lyophilized fractions were reconstituted in 10  $\mu$ l of 0.1% TFA, 50% acetonitrile; mixed with matrix solution; and applied to the MALDI target plate as described previously (18).

**MS Analysis of Cross-linked Peptides**—Mass spectrometric analyses were performed on a MALDI-TOF/TOF mass spectrometer (4700 Proteomics Analyzer, Applied Biosystems) operating in the reflectron mode. MALDI-MS spectra were screened for the presence of ion signal doublets/multiplets 8.05 and 4.03 Da apart. The screening and analysis of ion doublets was automated by means of a customized software program (isotopically coded cleavable cross-linking analysis software suite (ICC-CLASS)) developed in our laboratory (details to be published elsewhere).

Briefly the program consists of three modules. The first module, DXSet, searches the MS mass lists for presence of D<sub>8</sub> and D<sub>4</sub> peak doublets. The second module, DXDXMatch, looks for matches for the D<sub>4</sub> and D<sub>8</sub> peak doublets according to masses derived from equations describing the cleavage of different types of cross-links. The third module, DXMSMSMatch, performs the assignment of uncleaved and cleaved cross-links based on matching the isotopically coded cross-linker-containing and cross-linker-free fragment ion masses (from the MS/MS spectra mass lists) to the theoretically predicted fragment ion masses. The program is capable of automatic analysis of a set of multiple spots, for example, from an LC-MALDI analysis.

Doublet peak lists produced by the DXSet module can be downloaded as inclusion lists for automatic acquisition of the corresponding MSMS spectra, which in turn can be automatically analyzed by the DXMSMSMatch module. For the work described here, both doublet ions were simultaneously selected for tandem analysis by MALDI-TOF/TOF. For assignment of cross-linked peptides by mass, the MS-Bridge (Protein Prospector, Mass Spectrometry Facility, University of California San Francisco; bridge elemental composition for BiPS, C<sub>16</sub>H<sub>16</sub>N<sub>2</sub>O<sub>4</sub>S<sub>2</sub>) and ICC-CLASS programs were used to predict all possible combinations of cross-linked peptide masses. Fragment ions were manually matched to theoretical peptide fragments calculated by the MS-Product program (Protein Prospector, University of California San Francisco) and by the DXMSMSMatch module of ICC-CLASS.

**Molecular Modeling of the Phosphopeptide V<sub>2</sub>Rpp- $\beta$ -Arrestin Interaction Site**—We used Medusa (19–21), a general molecular modeling and design program, to determine the structure of the unbound state of the 29-mer synthetic phosphorylated peptide representing the C terminus of vasopressin type II receptor. Because the current version of Medusa contains no force field for phosphate groups, we substituted all the phosphorylated residues with glutamic acid to mimic the negatively charged phosphoryl groups. We also incorporated the distance constraints that represent known secondary structure information to force the sampled conformations to be consistent with the conserved secondary structure prediction by the PHD program (22). We performed a replica-exchange molecular dynamics simulation (23) with eight replicas at temperatures from 0.4 to 0.63 (temperature is in the unit of  $\epsilon/k_B$  where  $\epsilon$  is the energy unit and  $k_B$  is the Boltzmann constant) for 10<sup>5</sup> time units. These replica-exchange simulations were followed by annealing simulations of each replica for 10<sup>4</sup> time units to a temperature of 0.1. From eight annealing simula-

tions, we chose the conformations with the lowest energies, and that were consistent with the known secondary structure information.

Next we used a well established docking program, ZDOCK (24, 25), to determine the structure of the phosphopeptide- $\beta$ -arrestin complex based on the calculated structures of each component. Among the predicted structures for the complex, we chose the structure with the least violation of experimentally derived cross-linking constraints from the structures with the lowest energies as the structural template for further refinement. Finally we used Medusa to refine the predicted structure of the phosphopeptide- $\beta$ -arrestin complex so that the resulting structure of the complex satisfied all experimentally derived cross-linking constraints. In this complex, the phosphopeptide binds to the concave surface of the  $\beta$ -arrestin N-domain.

## RESULTS AND DISCUSSION

**Design and Analytical Characteristics of the Fluorescent, Photocleavable, and Isotopically Coded Cross-linker BiPS**—In previous studies, we found that the modification of cysteine residues by MBB, a commercially available fluorescent label for thiol groups, was partially reversible during MALDI-MS (10). Based on this finding, we synthesized a novel dibromobimane-derived cross-linker that is fluorescent and MALDI-MS photocleavable (Fig. 1A). The two bromine atoms of dibromobimane were reacted with thiol groups of mercaptopropionic acid, leading to the formation of thioesters of mercaptopropionic acid. To obtain a homobifunctional amino-reactive cross-linker, bimanedicarboxylic acid was activated with *N*-hydroxysuccinimide to form a di(*N*-hydroxysuccinimide) derivative that we call H<sub>8</sub>-BiPS (X = H in Fig. 1A). To facilitate the detection of the cross-linked peptides in the mass spectra, we also synthesized an isotopically labeled BiPS (D<sub>8</sub>-BiPS; X = D in Fig. 1A) derivative by using deuterated mercaptopropionic acid (*d*<sub>4</sub>-mercaptopropionic acid) synthesized from commercially available *d*<sub>4</sub>-bromopropionic acid. This D<sub>8</sub>-BiPS contains eight deuterium atoms in the aliphatic chain of the propionic acid portions of the molecule. The bimane moiety of BiPS gives rise to its fluorescent properties with excitation and emission maxima of 370 and 480 nm, respectively. Fluorescence provides much higher sensitivity than UV absorption and consequently can be used to facilitate the detection and separation of low-abundance cross-linked peptides. The maximum span of the cross-linker is 10 Å. The real spacing, however, was probably somewhat less because of the planar character of the bimane-fused heterocyclics.

**Characteristic Mass Spectrometric Signatures of MALDI-MS-induced Fragmentation of BiPS**—Based on previous observations, we predicted that MALDI conditions would lead to photoinduced cleavage of BiPS-cross-linked peptides in a manner analogous to MBB-modified cysteines. Fragmentation occurs at two specific sites that are adjacent to the sulfur atom (Fig. 1B). Photocleavage produces two halves of the cross-linked peptides, both of which are isotopically labeled with four deuterium atoms in the propionic acid moiety of the cross-linker. If a 1:1 mixture of H<sub>8</sub>-BiPS/D<sub>8</sub>-BiPS is used, this photocleavage generates ion signal doublets at a 1:1 ratio and

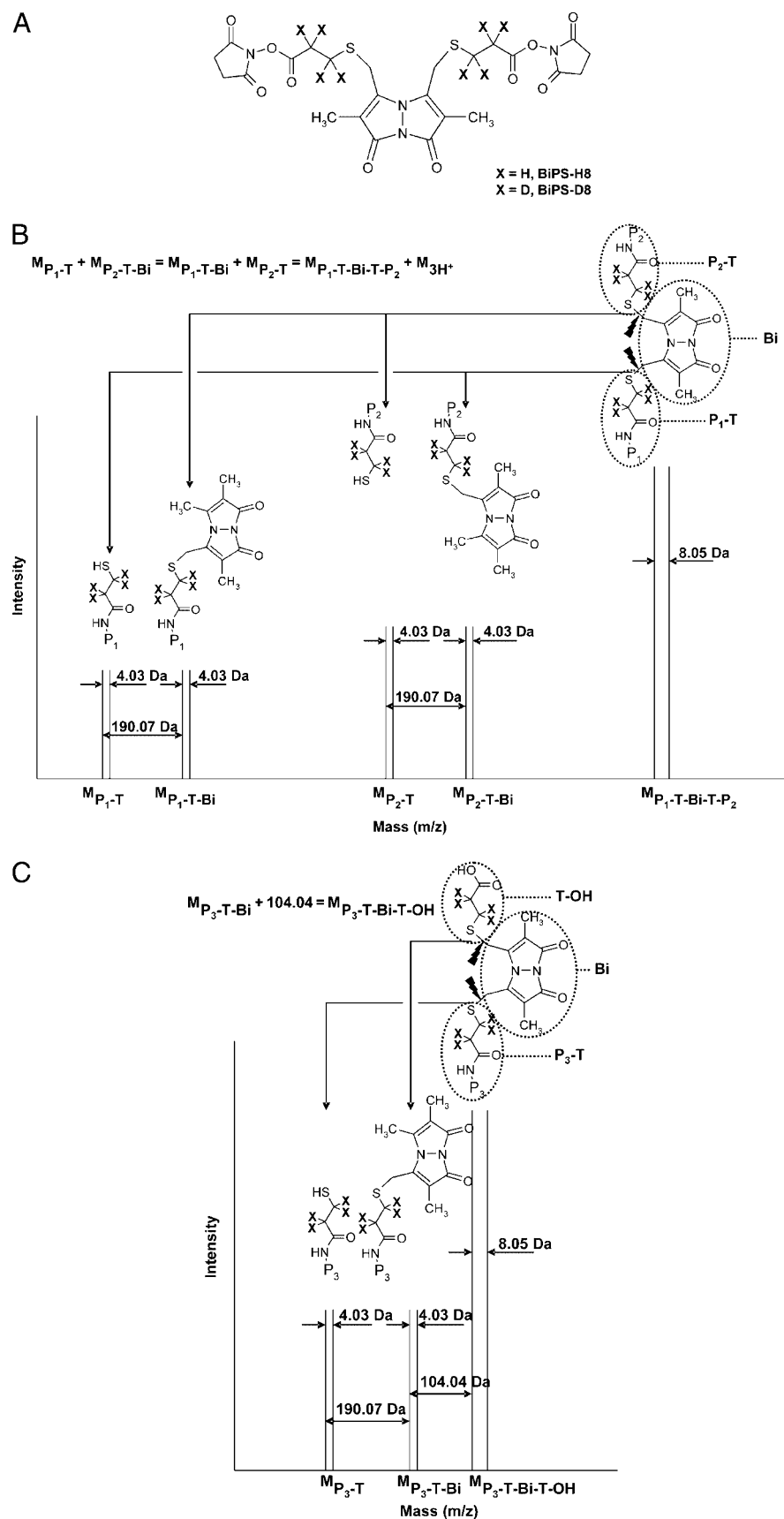


**FIG. 1. MALDI-induced photocleavage of BiPS in cross-links.** A, chemical structure of H<sub>8</sub>/D<sub>8</sub>-BiPS. B–D, scheme of the ion signals detectable in the MALDI-MS analysis of BiPS interpeptide (B), BiPS dead-end (C), and BiPS intra-peptide (D) cross-links. The ion signals are annotated by the chemical structures proposed for BiPS-containing peptides obtained after MALDI-induced fragmentation with thiopropionic (T), bi-mane (Bi), peptide (P), and hydroxyl (OH) moieties. “Lightning”-like arrows (↘) indicate sites of photocleavage. E, schematic of ICC-CLASS analysis using isotopic coding and cleavage features of BiPS.



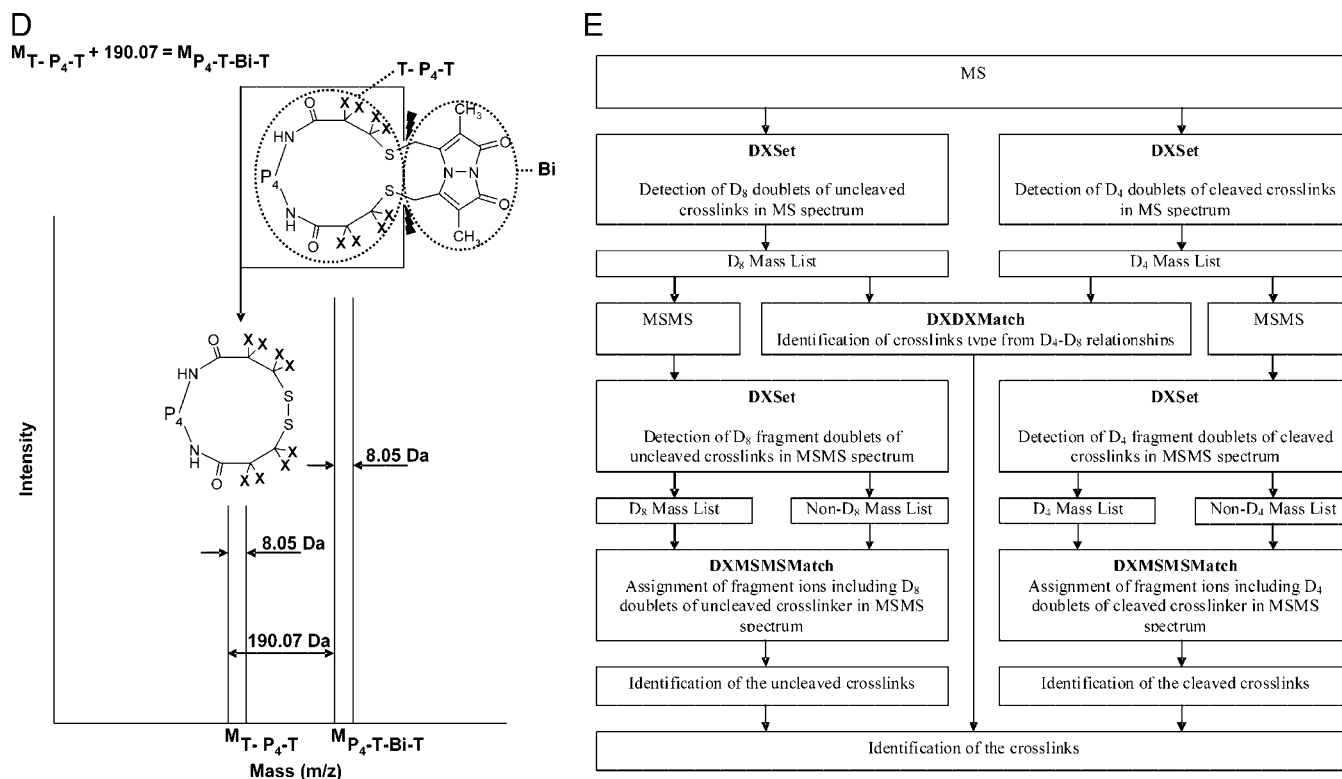


FIG. 1—continued

4.03 Da apart. Moreover because of the symmetrical nature of the cross-linker, the cleavage can occur with equal probability at either of the two sulfur atoms, thus producing two 4.03-Da doublets separated by a mass difference of 190.07 Da, a difference corresponding to the mass of the bimane moiety of the cross-linker.

As we demonstrated previously for the chemically cleavable, isotopically coded cross-linker  $D_{12}$ -EGSS (9), cross-linker cleavage facilitates analysis of the cross-linked peptides. Cleavage enables the researcher to distinguish between different types of cross-links (dead end, intra-, or interpeptide). Most importantly, cross-linker cleavage permits accurate mass determination and sequence analysis of the individual peptides constituting the cross-link, thus facilitating identification of cross-linked peptides and cross-linking sites. All of these benefits are provided by the photoinducible cleavage of BiPS. Moreover because the cleavage occurs during MALDI-MS, sample loss is negligible. This is in contrast to *chemical* cross-linker cleavage, which is typically not performed *in situ* and requires an additional purification step that may lead to sample loss.

Dead-end BiPS cross-links can be assigned based on the occurrence of two 4.03-Da ion doublets that are 104 and 294 Da lower than the mass of the 8.05-Da doublet of the non-cleaved cross-links (Fig. 1C). Individual peptides derived from cleavage of BiPS interpeptide cross-links appear as doublets

separated by 4.03 Da with the  $m/z$  values of the singly charged modified peptide equal to the mass of the unmodified uncharged peptide plus 89 and/or 279 Da.

According to our studies on  $H_8$ -BiPS/ $D_8$ -BiPS-cross-linked peptides (data not shown), photocleavage of intrapeptide cross-links results in the formation of a disulfide-containing peptide that occurs as an 8.05-Da ion doublet that is 190 Da lower in mass than the intrapeptide cross-link (Fig. 1D). The masses of individual peptides obtained by photocleavage are related to the mass of the original non-cleaved cross-link according to the equations shown in Fig. 1, B–D. These mathematical relationships provide further verification of assigned cross-link types.

Recently we developed a simple-to-use software algorithm for automatic detection and identification of  $H_{12}$ -EGSS/ $D_{12}$ -EGSS cross-link types (9). Based on this algorithm, we developed a software package called ICC-CLASS to carry out fully automated detection and assignment of isotopically coded cleavable dead-end, intra-, and interpeptide cross-links (Fig. 1E). The ICC-CLASS program can also generate lists of masses, including BiPS-containing uncleaved and cleaved cross-links, and these lists can be downloaded for automated MS/MS acquisition on a MALDI-TOF/TOF instrument. Moreover ICC-CLASS is capable of analyzing and interpreting MS/MS spectra by assigning fragment ions from isotopically coded cross-links from protein complexes to known se-

quences. When combined with GPS Explorer™ or Mascot analysis of MS/MS data for individual peptides obtained after cross-linker cleavage, ICC-CLASS can be used to identify unknown dead-end, inter-, and intrapeptide cross-links. This program is designed as an integrated software/instrument platform allowing a completely automated and targeted analysis of isotopically coded cross-links from data acquisition by MALDI-MS and -MS/MS to the assignment and identification of the cross-links.

**Model Protein Complex RNase S**—To evaluate the applicability of BiPS and ICC-CLASS to protein cross-linking studies, we cross-linked the model complex RNase S, a small protein heterodimer consisting of a 20-mer S-peptide and a 14-kDa core protein. The cross-linking was performed with a 1:1 mixture of H<sub>8</sub>-BiPS and D<sub>8</sub>-BiPS, the reaction was quenched with ammonium bicarbonate, and the components were separated by SDS-PAGE. Protein bands containing BiPS can be conveniently visualized under UV light with a standard UV light box typically used for ethidium bromide-stained DNA agarose gels (Fig. 2A).

The upper band in Fig. 2A corresponds to the BiPS-cross-linked complex, whereas the lower band represents dead-end derivatives of the RNase S core. The upper band was subjected to in-gel proteolytic digestion, and the extracted peptides were separated using reversed-phase HPLC with fluorescence detection (Fig. 2B). It is worth noting that the degree of completeness of the digestion can be determined by monitoring the fluorescence of the extracted peptides compared with the residual fluorescence of the protein band in the gel.

Although the UV absorbance of the peptides during HPLC was practically undetectable (data not shown), the fluorescence chromatogram did reveal the target cross-linked peptides (Fig. 2B). The small volume of sample required and increased sensitivity of fluorescence detection *versus* UV detection are compatible with nano-LC. This can make BiPS cross-linking suitable for electrospray LC-MS approaches with on-line fluorescence detection. On-line fluorescence detection could be used to develop a sensitive and accurate quantitative and qualitative analysis in which fluorescence-dependent MS/MS acquisition could be used for selective analysis of BiPS-containing peptides. This highly sensitive and quantitative method could be useful in probing changes in protein structure, including the detection of minor conformational alterations of potential biological significance.

For off-line separation, MALDI-MS is advantageous because of the partial cleavage of BiPS under MALDI-MS conditions and the capacity for reanalysis of the same sample spots. Fig. 2C depicts the MALDI spectrum of a fluorescent fraction from an HPLC separation of cross-linked RNase S after proteolysis. Two BiPS-containing peptides and their associated photocleaved fragmentation products are indicated by two doublets 8.05 Da apart (at  $m/z$  1256.73 and  $m/z$  1532.88) and four doublets 4.03 Da apart, respectively. ICC-CLASS assigned the doublet at  $m/z$  1256.73 as an interpep-

tide cross-link, whereas the doublet at  $m/z$  1532.88 was assigned as a dead-end cross-link based on the specific MS signatures of the cross-link types (see above). MS/MS analysis of the peptides induced by photocleavage of the cross-linker followed by computerized assignment of the sequence-specific ions via ICC-CLASS provided unambiguous identification of the BiPS-cross-linked peptides (Fig. 2D and Table I).

Detailed examination of the x-ray crystallographic structure of RNase S S-protein and S-peptide binding sites revealed that the structural information obtained from the cross-linked peptides agrees well with our protein-protein interaction site data because the distances between cross-linked sites are within the maximum span of the cross-linker (26). Thus, these experiments demonstrate the feasibility of using BiPS to structurally characterize protein-protein interaction sites as well as the capability of ICC-CLASS to facilitate detection, assignment, and identification of cross-links.

**Protein-Protein Interaction of the Vasopressin Receptor C Terminus and  $\beta$ -Arrestin 1**—We next applied this methodology to the elucidation of the protein-protein interaction site between vasopressin type II receptor (V<sub>2</sub>R), a member of the seven transmembrane-spanning G-protein-coupled receptor family, and its adaptor,  $\beta$ -arrestin. Previously we developed an *in vitro* receptor- $\beta$ -arrestin interaction model using a 29-mer synthetic multiposphopeptide (V<sub>2</sub>Rpp) derived from the phosphorylated C terminus of V<sub>2</sub>R. We demonstrated that V<sub>2</sub>Rpp bound to  $\beta$ -arrestin and simulated the effects of an activated phosphorylated GPCR, whereas the corresponding nonphosphorylated peptide, V<sub>2</sub>Rnp, had no effect (16). This *in vitro* model represents a simplified receptor- $\beta$ -arrestin interaction system in which the binding site for the V<sub>2</sub>Rpp on  $\beta$ -arrestin represents that for the phosphorylated C terminus of the receptor.

To locate the binding site of V<sub>2</sub>Rpp on  $\beta$ -arrestin,  $\beta$ -arrestin 2 was cross-linked with and without V<sub>2</sub>Rpp using a 1:1 mixture of H<sub>8</sub>-BiPS and D<sub>8</sub>-BiPS. Reaction mixtures were digested with trypsin, the resulting peptides were separated by reversed-phase HPLC with on-line fluorescence detection, and the fluorescent fractions were analyzed by MALDI-MS and MALDI-MS/MS (Table II, part A). Alternatively cross-linked reaction mixtures of  $\beta$ -arrestin 1 with V<sub>2</sub>Rpp or V<sub>2</sub>Rnp were separated by SDS-PAGE, and the protein bands were excised and in-gel digested with trypsin. The resulting tryptic peptides were analyzed by MALDI-MS and MALDI-MS/MS (Table II, part B).

The utility of this methodology is shown in Fig. 3, A and B. Although the MS spectrum shows numerous ion signals, the ICC-CLASS program detected doublets of ion signals 8.05 Da apart that correspond to the interpeptide cross-link as well as doublets 4.03 Da apart that represent individual peptides released by MALDI photocleavage of the cross-link. No  $\beta$ -arrestin-V<sub>2</sub>Rnp interpeptide cross-link was observed when the corresponding non-phosphorylated peptide, V<sub>2</sub>Rnp, was

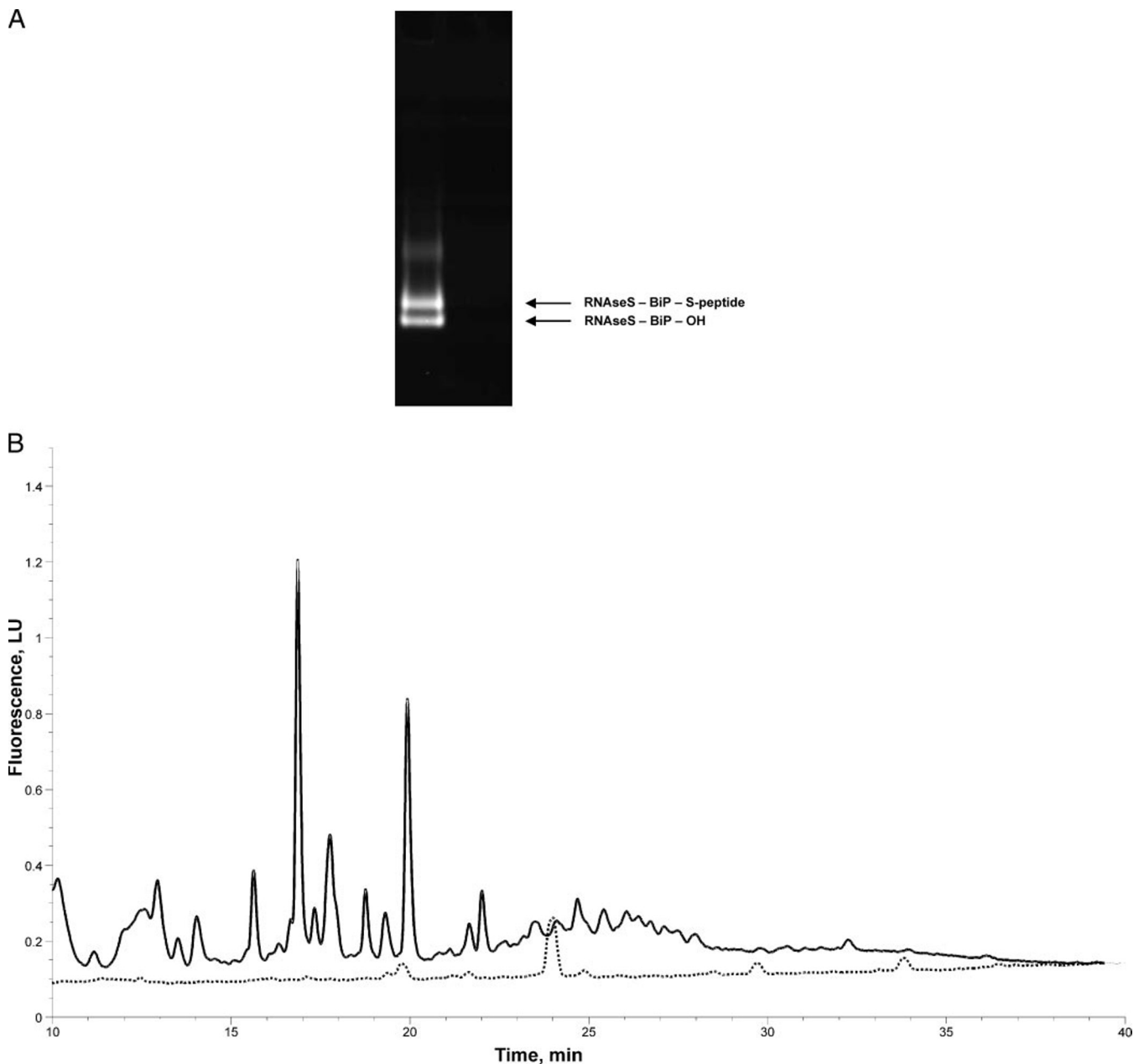
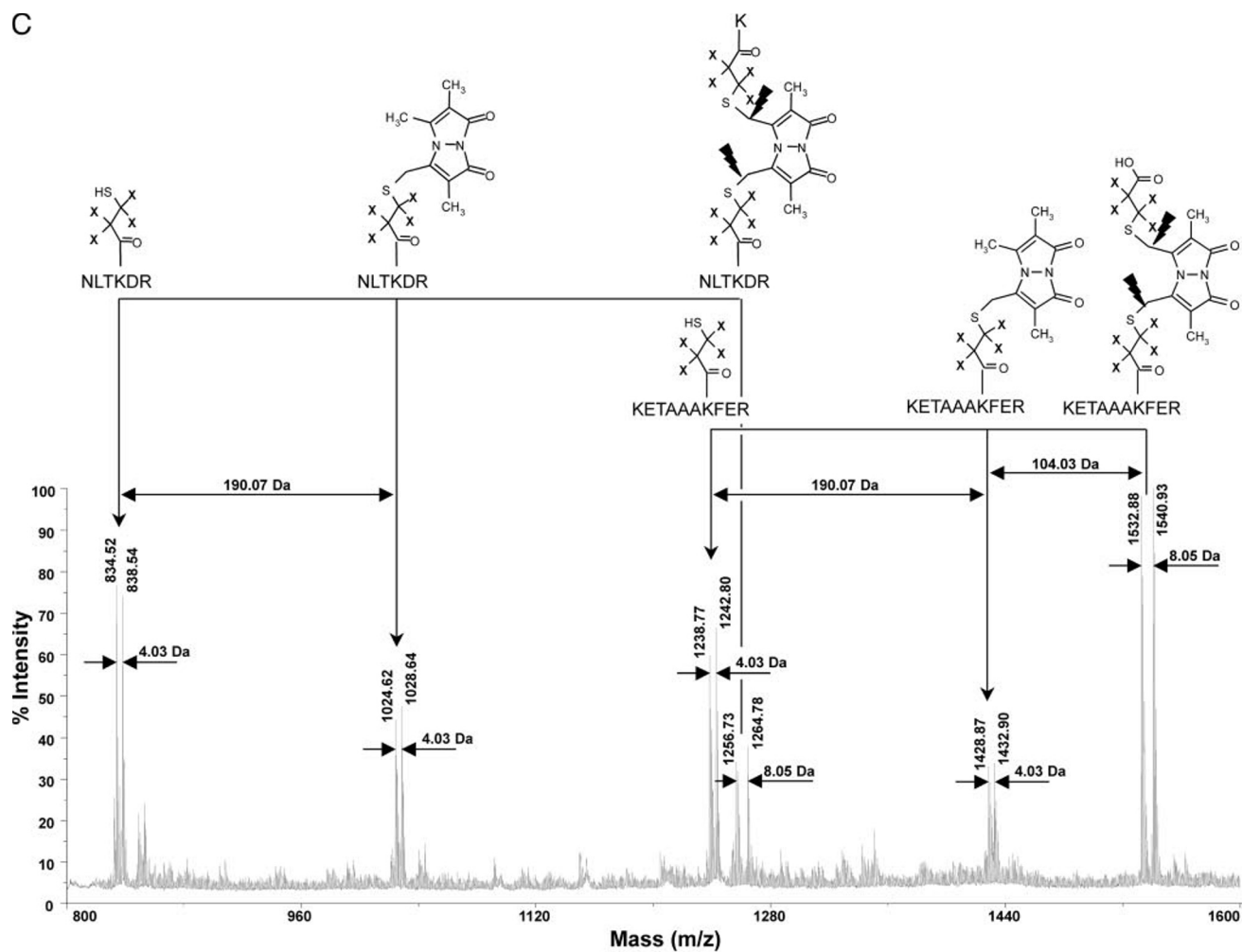


**FIG. 2. BiPS cross-linking followed by MALDI-MS analysis using RNase S heterodimer as a model complex.** *A*, gel image under UV illumination from SDS-PAGE analysis of RNase S after cross-linking with BiPS. The *upper* fluorescent band relates to the heterodimer of RNase S cross-linked by BiPS. *B*, HPLC with fluorescence detection (excitation, 370 nm; emission, 480 nm) of BiPS-cross-linked RNase S after SDS-PAGE separation of the cross-linked complex followed by in-gel digestion with trypsin. The *dotted line* corresponds to the fluorescence chromatogram of HPLC analysis of a blank piece of gel after in-gel digestion as a negative control. *C*, MALDI-MS analysis of a fluorescent HPLC fraction containing BiPS interpeptide and dead-end peptide cross-links of RNase S. The ion signals are annotated with  $m/z$  values and assigned to BiPS-containing peptides and photolysis products of BiPS cross-links, based on their mass, doublet formation, and masses relative to other doublets of ion signals. *D*, MS/MS analysis of the ion doublet with  $m/z$  834.52 and 838.54. The sequence-specific b- and y-ions are assigned, resulting in complete sequencing of the peptide representing the BiPS interpeptide cross-links of RNase S released by photocleavage of the cross-linker. *LU*, luminescence units.

used (data not shown). Subsequent MS/MS analysis of the peptides constituting the cross-link allowed unambiguous identification of the cross-link site (Fig. 3*B*). These results demonstrate an interaction between the N terminus of V<sub>2</sub>Rpp and lysine 85 of  $\beta$ -arrestin 1 that is located in  $\beta$ -sheet VII of the

N-domain. Further support for this interaction was provided by additional interpeptide cross-links between the N terminus of V<sub>2</sub>Rpp and lysine 11 of  $\beta$ -arrestin 2 that were also assigned and identified using the ICC-CLASS software (Table II, part A). These data are in agreement with the current receptor-arrestin

C



D

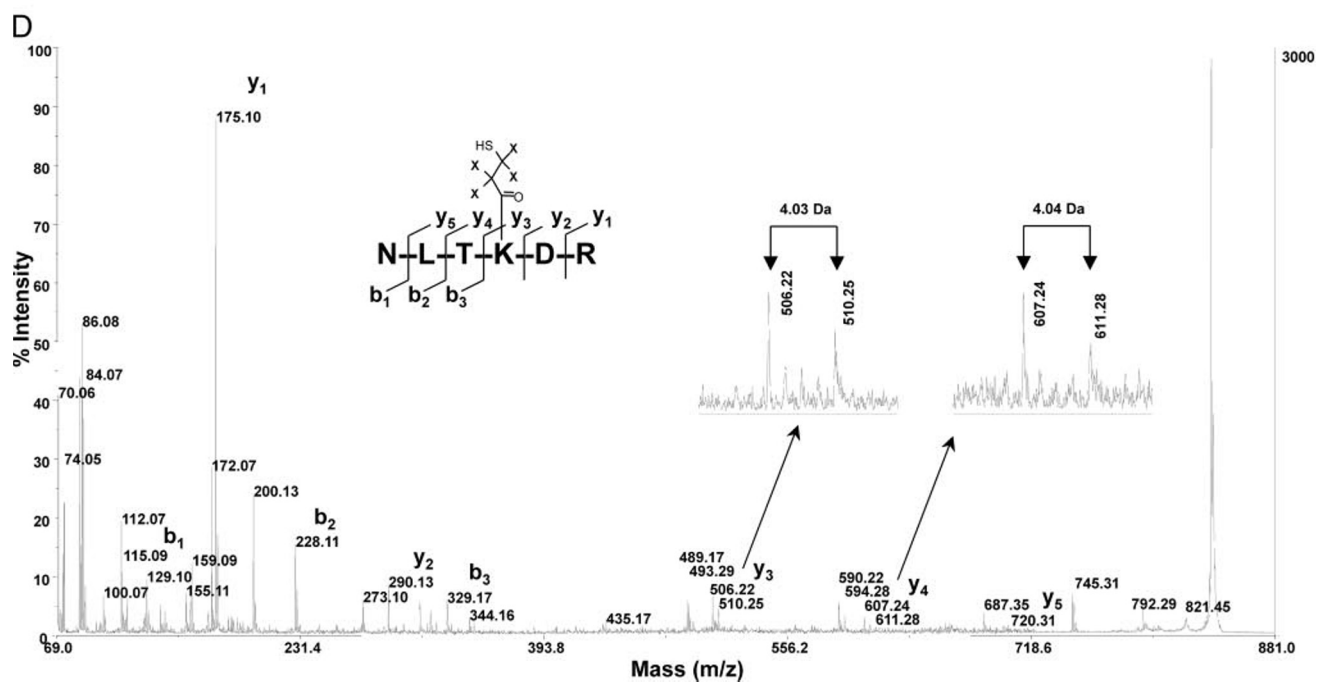


FIG. 2—continued



TABLE I  
RNase S BiPS cross-links

Assigned tryptic cross-links from HPLC fractions 13–36 of in-gel tryptic digest of BiPS-cross-linked RNase S are shown.  $D_{8\text{ obs}}$  and  $D_{8\text{ calc}}$ , observed and calculated  $D_8$  peak doublets, respectively;  $\Delta D_8$ , mass error for  $D_8$  peak doublets ( $\Delta D_8 = M_{D_8} - M_{H_8} - 8.05021\text{ Da}$ ); CL type, cross-link type (i, intrapeptide; OH and  $\text{NH}_2$ , carboxyl and amide dead end, respectively; ip, interpeptide); C, protein chain of RNase S; Sr, starting peptide amino acid residue; Er, ending peptide amino acid residue;  $D_{4\text{ obs}}$  and  $D_{4\text{ calc}}$ , observed and calculated  $D_4$  peak doublets of photocleaved products, respectively;  $\Delta D_4$ , mass error for  $D_4$  peak doublets ( $\Delta D_4 = M_{D_4} - M_{H_4} - 4.02511\text{ Da}$ ); T, thiopropionic moieties of the cross-linker; Bi, bimanine moieties of the cross-linker (see Fig. 1). Residues in parentheses represent residues preceding and following the enzymatic digestion site. Dashes in parentheses correspond to the N or C terminus.

$D_{8\text{ obs}}$	$D_{8\text{ calc}}$	$\Delta D_8$	CL type	C	Sr	Er	Sequence	$D_{4\text{ obs}}$	$D_{4\text{ calc}}$	$\Delta D_4$	Cleaved products
Da	Da	Da						Da	Da	Da	
1082.60	1082.46	0.00	i	1	1	7	(-)KETAAAK(F)		892.39 <sup>a</sup>		1T-T
1100.62	1100.48	0.00	1-OH	1	1	7	(-)KETAAAK(F)		806.41		1T
								996.63	996.48	-0.04	1T-Bi
1127.68	1127.50	0.00	1-NH <sub>2</sub>	2	14	19	(R)NLTKDR(C)	834.55	834.41	0.00	1T
								1024.65	1024.49	0.00	1T-Bi
1128.65	1128.48	0.00	1-OH	2	14	19	(R)NLTKDR(C)	834.55	834.41	0.00	1T
								1024.64	1024.49	0.00	1T-Bi
1256.74	1256.58	0.00	ip	2	14	19	(R)NLTKDR(C)	834.53	834.41	0.00	1T
								1024.62	1024.49	0.00	1T-Bi
				1	1	1	(-)K(E)		235.11		1T
									425.19		1T-Bi
1403.83	1403.61	0.00	1-NH <sub>2</sub>	1	2	10	(K)ETAAAKFER(Q)	1110.69	1110.52	0.00	1T
								1300.79	1300.60	0.00	1T-Bi
1404.80	1404.59	0.00	1-OH	1	2	10	(K)ETAAAKFER(Q)	1110.68	1110.52	0.00	1T
								1300.78	1300.60	0.00	1T-Bi
1482.77	1482.54	0.00	2-OH	1	1	7	(-)KETAAAK(F)		894.41		2T
								1084.64	1084.48	0.01	1T, 1T-Bi
									1274.55		2T-Bi
									1188.47		1T, 1T-Bi-T-OH
								1378.83	1378.55	-0.05	1T-Bi, 1T-Bi-T-OH
1514.90	1514.68	0.00	i	1	1	10	(-)KETAAAKFER(Q)	1324.79 <sup>a</sup>	1324.60 <sup>a</sup>	0.00	1T-T
1532.88	1532.69	0.00	1-OH	1	1	10	(-)KETAAAKFER(Q)	1238.77	1238.62	0.00	1T
								1428.87	1428.69	0.00	1T-Bi
1828.92	1828.73	-0.02	1-NH <sub>2</sub>	2	66	78	(R)ETGSSSKYPNCAYK(T)		1535.65		1T
									1725.72		1T-Bi
1830.00	1829.72	-0.02	1-OH	2	66	78	(R)ETGSSSKYPNCAYK(T)	1535.85	1535.65	0.02	1T
								1725.99	1725.72	0.01	1T-Bi
1883.07	1882.79	0.02	1-NH <sub>2</sub>	2	72	84	(K)YPNCAYKTTQANK(H)	1589.93	1589.71	0.00	1T
									1779.78		1T-Bi
1884.07	1883.78	-0.01	1-OH	2	72	84	(K)YPNCAYKTTQANK(H)	1589.93	1589.71	-0.01	1T
								1780.03	1779.78	0.00	1T-Bi
1897.03	1896.74	0.00	i, 1-OH	1	1	10	(-)KETAAAKFER(Q)	1412.85	1412.60	-0.03	1T-T, 1T
								1602.92	1602.67	-0.02	1T-T, 1T-Bi; 1T-Bi-T, 1T
								1706.94	1706.67	-0.01	1T-T, 1T-Bi-T-OH
								1793.01	1792.75	0.00	1T-Bi-T, 1T-Bi
1899.98	1899.70	-0.01	i	2	1	13	(-)SSSNYCNQMMKSR(N)		1709.62 <sup>a</sup>		1T-T
1812.93	1812.66	-0.01	i	2	2	13	(-)SSSNYCNQMMKSR(N)		1622.59 <sup>a</sup>		1T-T
1915.02	1914.75	-0.02	2-OH	1	1	10	(-)KETAAAKFER(Q)		1326.62		2T
									1516.69		1T, 1T-Bi
									1706.77		2T-Bi
								1620.92	1620.69	-0.03	1T, 1T-Bi-T-OH
								1811.01	1810.76	-0.02	1T-Bi, 1T-Bi-T-OH
1918.03	1917.71	-0.01	1-OH	2	1	13	(-)SSSNYCNQMMKSR(N)	1623.92	1623.64	-0.01	1T
								1814.01	1813.71	0.00	1T-Bi
2624.58	2624.14	-0.06	i, ip	1	1	10	(-)KETAAAKFER(Q)	1412.84	1412.60	-0.02	1T-T, 1T
								1602.92	1602.67	-0.01	1T-T, 1T-Bi; 1T-Bi-T, 1T
								2434.15	2434.07	-0.03	1T-T, 1T-Bi-T-P2
								1793.01	1792.75	0.00	1T-Bi-T, 1T-Bi
				2	14	19	(R)NLTKDR(C)	834.55	834.41	0.00	1T
								1024.64	1024.49	-0.01	1T-Bi

<sup>a</sup>  $D_8$  peak doublet, cleaved products as in Fig. 1.

TABLE II  
*V<sub>2</sub>R phosphopeptide-β-arrestin BiPS cross-links*

Part A, assigned tryptic cross-links from HPLC fractions 13–36 of in-solution tryptic digest of BiPS-cross-linked *V<sub>2</sub>Rpp-β-arrestin 2*. Part B, assigned tryptic cross-links from in-gel digest of BiPS-cross-linked *V<sub>2</sub>Rpp-β-arrestin 1*. Abbreviations are the same as in Table I. Residues in parentheses represent residues preceding and following the enzymatic digestion site. Dashes in parentheses correspond to the N or C terminus.

D <sub>8 obs</sub>	D <sub>8 calc</sub>	ΔD <sub>8</sub>	CL type	C	Sr	Er	Sequence	D <sub>4 obs</sub>	D <sub>4 calc</sub>	ΔD <sub>4</sub>	Cleaved products
<i>Da</i>	<i>Da</i>	<i>Da</i>						<i>Da</i>	<i>Da</i>	<i>Da</i>	
A											
902.41	902.43	0.00	1-NH <sub>2</sub>	1	16	19	(R)VFKK(S)	609.29	613.34	0.02	1T
								799.37	799.42	0.02	1T-Bi
903.42	903.41	0.00	1-OH	1	16	19	(R)VFKK(S)	609.34	609.34	0.00	1T
								799.41	799.42	0.00	1T-Bi
908.40	908.39	0.00	1-NH <sub>2</sub>	1	166	169	(K)SHKR(N)	615.30	615.30	0.01	1T
								805.39	805.38	0.00	1T-Bi
909.35	909.37	0.00	1-OH	1	166	169	(K)SHKR(N)	615.29	615.30	0.00	1T
								805.35	805.38	-0.01	1T-Bi
958.45	958.42	0.00	1-OH	1	404	408	(R)LKGMK(D)		664.35		1T
									854.43		1T-Bi
998.40	998.38	0.00	1-NH <sub>2</sub>	1	1	6	(-)GSPNSR(V)	705.31	705.30	0.00	1T
								895.38	895.37	0.01	1T-Bi
999.35	999.37	0.00	1-OH	1	1	6	(-)GSPNSR(V)	705.26	705.30	0.00	1T
								895.33	895.37	0.00	1T-Bi
1144.40	1144.46	-0.01	1-NH <sub>2</sub>	1	19	25	(K)KSPNCK(L)	851.34	851.38	0.01	1T
								1041.36	1041.45	-0.04	1T-Bi
1182.64	1182.60	0.00	1-OH	1	334	340	(K)VKLVS(R)		888.53		1T
								1078.43	1078.61	-0.07	1T-Bi
1296.57	1296.68	-0.03	ip	1	292	294	(R)EKR(G)	520.29	520.26	-0.03	1T
									710.33		1T-Bi
				1	112	115	(R)LLKK(L)		589.37		1T
									779.45		1T-Bi
1331.66	1331.65	0.00	1-OH	1	26	33	(K)LTIVYLGR(D)	1037.60	1037.58	-0.01	1T
								1227.67	1227.66	0.00	1T-Bi
1339.56	1339.58	0.00	1-NH <sub>2</sub>	1	7	15	(R)VDGEKPGTR(V)	1046.48	1046.49	0.00	1T
								1236.55	1236.57	0.00	1T-Bi
1340.54	1340.56	0.00	1-OH	1	7	15	(R)VDGEKPGTR(V)	1046.48	1046.49	0.00	1T
								1236.55	1236.57	0.00	1T-Bi
1357.74	1357.74	-0.09	ip	1	332	335	(R)VKVK(L)		561.34		1T
									751.42		1T-Bi
				1	16	19	(R)VFKK(S)	609.34	609.34	0.00	1T
								799.41	799.42	0.00	1T-Bi
1411.60	1411.70	-0.02	ip	1	16	19	(R)VFKK(S)		609.34		1T
								799.31	799.42	0.00	1T-Bi
				1	166	169	(K)SHKR(N)	615.29	615.30	0.00	1T
								805.35	805.38	-0.01	1T-Bi
1501.68	1501.69	0.00	ip	1	16	19	(R)VFKK(S)	609.29	609.34	0.03	1T
								799.34	799.42	0.03	1T-Bi
				1	1	6	(-)GSPNSR(V)	705.26	705.30	0.00	1T
								895.33	895.37	0.00	1T-Bi
1567.70	1567.70	-0.03	ip	2	1	2	(-)AR(G)		334.15		1T
								524.22	524.23	0.00	1T-Bi
				1	7	15	(R)VDGEKPGTR(V)	1046.47	1046.49	0.00	1T
								1236.54	1236.57	-0.01	1T-Bi
1791.77	1791.81	0.00	1-OH	1	20	32	(K)SSPNCKLTIVYLGR(R)	1497.71	1497.74	-0.01	1T
								1687.83	1687.82	-0.02	1T-Bi
1822.92	1822.92	0.00	ip	1	112	115	(R)LLKK(L)		589.37		1T
									779.45		1T-Bi
				1	7	15	(R)VDGEKPGTR(V)	1046.49	1046.49	0.02	1T
								1236.56	1236.57	-0.01	1T-Bi
1842.85	1842.89	0.00	ip	1	16	19	(R)VFKK(S)	609.29	613.34	0.02	1T
								799.37	799.42	0.02	1T-Bi
				1	7	15	(R)VDGEKPGTR(V)	1046.46	1046.49	0.00	1T
								1236.52	1236.57	0.00	1T-Bi

TABLE II—continued

D <sub>8 obs</sub>	D <sub>8 calc</sub>	ΔD <sub>8</sub>	CL type	C	Sr	Er	Sequence	D <sub>4 obs</sub>	D <sub>4 calc</sub>	ΔD <sub>4</sub>	Cleaved products
<i>Da</i>	<i>Da</i>	<i>Da</i>						<i>Da</i>	<i>Da</i>	<i>Da</i>	
<b>A</b>											
1877.78	1877.73	0.00	2-OH	1	161	169	(K)SIEEKSHKR(N)	1289.58	1289.60	0.06	2T
								1479.72	1479.67	−0.01	1T, 1T-Bi
								1669.76	1669.75	0.00	2T-Bi
								1583.71	1583.67	0.00	1T, 1T-Bi-T-OH
								1773.78	1773.74	0.01	1T-Bi, 1T-Bi-T-OH
1938.84	1938.84	0.00	ip	1	1	6	(−)GSPNSR(V)	705.30	705.30	0.00	1T
								895.37	895.37	0.00	1T-Bi
				1	7	15	(R)VDGEKPGTR(V)	1046.50	1046.49	0.00	1T
								1236.57	1236.57	0.00	1T-Bi
2295.05	2295.04	0.00	1-NH <sub>2</sub>	1	304	321	(K)HEDTNLASSTIVKEGANK(E)	2002.00	2001.96	−0.02	1T
								2192.03			1T-Bi
2423.14	2423.10	0.02	1-OH	1	178	196	(R)KVQFAPETPGPQPSAETTR(H)	2129.08	2129.03	−0.02	1T
								2319.11			1T-Bi
2459.13	2459.15	−0.04	1-OH	1	7	25	(R)VDGEKPGTRVFKKSSPNCK(L)	2165.03	2165.08	0.00	1T
								2355.11	2355.16	−0.01	1T-Bi
2691.32	2691.31	−0.02	1-NH <sub>2</sub>	1	295	316	(R)GLALDGQLKHEDTNLASSTIVK(E)	2398.23	2398.23	0.00	1T
								2588.30	2588.30	−0.01	1T-Bi
2692.28	2692.30	0.00	1-OH	1	295	316	(R)GLALDGQLKHEDTNLASSTIVK(E)	2398.20	2398.23	−0.01	1T
								2588.28	2588.30	−0.01	1T-Bi
3105.58	3105.53	−0.01	ip	1	292	294	(R)EKR(G)	520.27	520.26	−0.03	1T
								710.34	710.33	−0.01	1T-Bi
				1	295	316	(R)GLALDGQLKHEDTNLASSTIVK(E)	2398.21	2398.23	0.00	1T
								2588.35	2588.30	−0.03	1T-Bi
<b>B</b>											
1227.47	1227.49	−0.01	1NH <sub>2</sub>	1	1	8	(−)GSPEFPGR(L)	934.40	934.41	−0.01	1T
								1124.46	1124.48	0.00	1T-Bi
1228.46	1228.48	0.00	1OH	1	1	8	(−)GSPEFPGR(L)	934.40	934.41	−0.01	1T
								1124.46	1124.48	0.00	1T-Bi
1331.53	1331.65	0.02	1OH	1	26	33	(K)LTVYLGKR(D)	1037.53	1037.58	0.05	1T
								1227.61	1227.66	0.01	1T-Bi
1833.86	1833.98	−0.01	ip	1	16	19	(R)VFKK(A)		609.34		1T
									799.42		1T-Bi
				1	26	33	(K)LTVYLGKR(D)	1037.53	1037.58	0.05	1T
								1227.61	1227.66	0.01	1T-Bi
1955.85	1955.87	0.01	ip	1	9	15	(R)LGDKGTR(V)	834.41	834.41	−0.01	1T
								1024.47	1024.49	0.00	1T-Bi
				1	1	8	(−)GSPEFPGR(L)	934.40	934.41	−0.01	1T
								1124.46	1124.48	0.00	1T-Bi
2383.09	2383.11	0.01	1NH <sub>2</sub>	1	85	102	(R)KDLFVANVQSFPAPEDK(K)	2090.00	2090.03	0.00	1T
								2280.08	2280.10	0.02	1T-Bi
2611.22	2611.23	0.00	ip	2	1	2	(−)AR(G)		334.15		1T
								524.33	524.23	0.00	1T-Bi
				1	85	102	(R)KDLFVANVQSFPAPEDK(K)	2090.00	2090.03	0.00	1T
								2280.08	2280.10	0.02	1T-Bi
3378.60	3378.59	−0.02	1OH	1	34	59	(R)DFVDHIDLVPDGVVLVDPEYLKER(R)	3084.52	3084.52	−0.04	1T
								3274.58	3274.60	0.00	1T-Bi

interaction model (27) and provide the first direct experimental evidence for the location of the binding site of the C terminus of GPCR to the  $\beta$ -arrestin molecule.

To further characterize the protein-protein interaction site, we computationally predicted the secondary structure of the 29-mer phosphopeptide that represents the C terminus of V<sub>2</sub>R. Using the x-ray structure of  $\beta$ -arrestin, we then used molecular modeling programs to compute the structure of the phosphopeptide- $\beta$ -arrestin complex by utilizing experimentally derived cross-linking constraints (Fig. 3C). The computed

structure of the complex shows that V<sub>2</sub>Rpp binds to the concave surface of the  $\beta$ -arrestin N-domain.

By using a methodology combining MS and our BiPS cross-linker, we successfully mapped the binding site of a receptor C terminus on the multifunctional scaffold and adaptor protein  $\beta$ -arrestin, thus paving the way toward elucidating the structural basis of this dynamic receptor- $\beta$ -arrestin interaction. Our findings will aid in the understanding not only of the regulatory mechanism of a wide variety of GPCR-mediated physiological cellular processes but also of the molecular

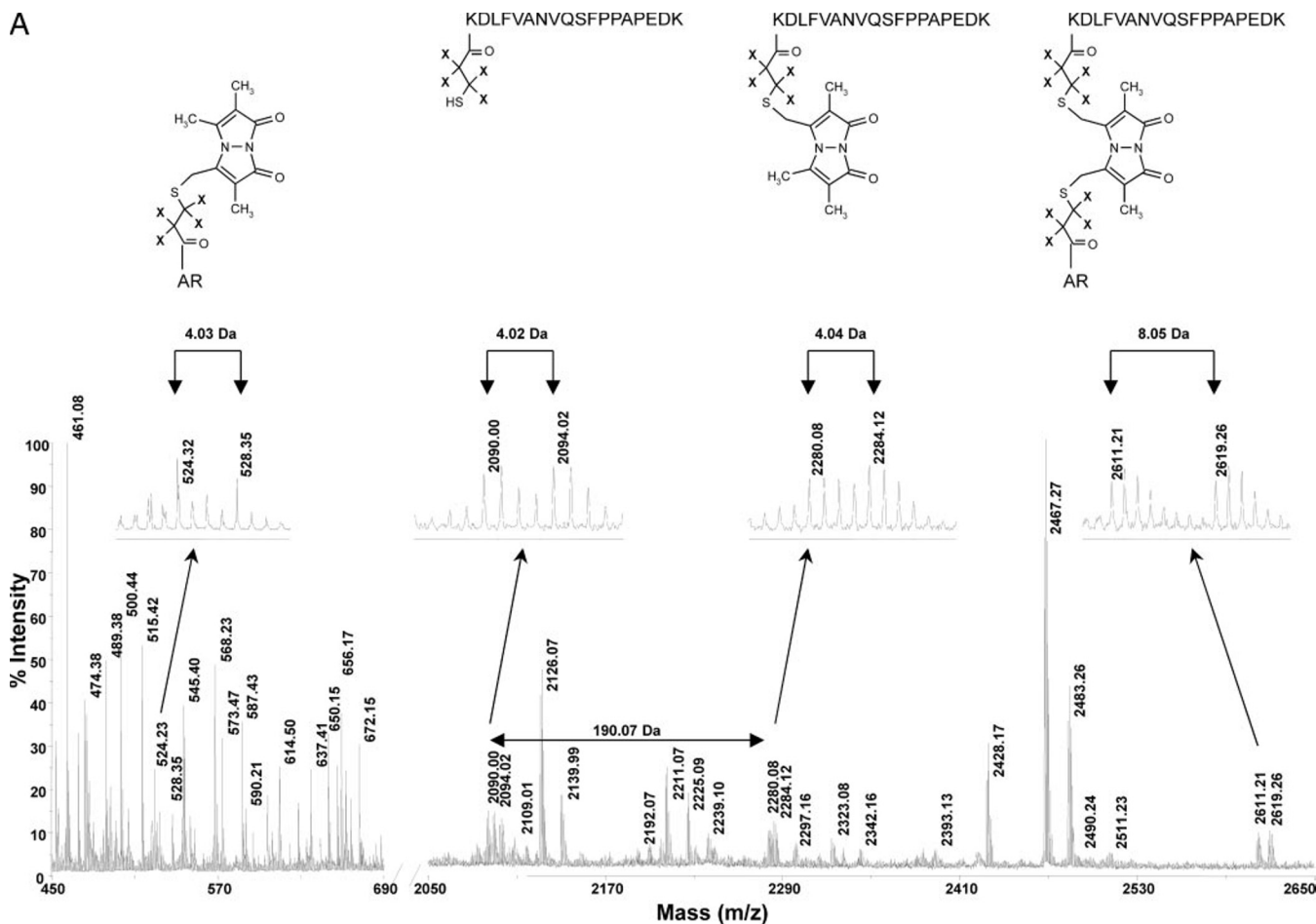


**FIG. 3. Identification of the V<sub>2</sub>R C terminus binding site on  $\beta$ -arrestin by BiPS cross-linking.** A, MALDI-MS analysis of a BiPS interpeptide cross-link, V<sub>2</sub>R phosphopeptide- $\beta$ -arrestin 1. BiPS cross-links lysine 85 of the tryptic peptide (<sup>85</sup>KDLFVANVQSFPAPEDK<sup>102</sup>) from  $\beta$ -arrestin 1 and the N-terminal alanine of the tryptic peptide (<sup>1</sup>AR<sup>2</sup>) from V<sub>2</sub>Rpp. The doublet peaks of the interpeptide and its photocleaved products are enlarged and shown in the insets. B, tandem mass spectra of the individual peptides released by photocleavage of the interpeptide cross-link. C, location and modeling of the interaction site of V<sub>2</sub>R phosphopeptide- $\beta$ -arrestin. Shown is the predicted structure of the V<sub>2</sub>R phosphopeptide- $\beta$ -arrestin complex computed by molecular modeling to fit the constraints of the experimentally identified interaction between the N terminus of the V<sub>2</sub>R phosphopeptide and  $\beta$ -arrestins.

basis of numerous clinical diseases associated with dysregulation of GPCR signaling.

**Conclusions**—In conclusion, we report here the synthesis and application of the novel cross-linker BiPS. BiPS is distinguished from other reagents by a unique combination of chemical groups that render it homobifunctional, amine-reactive, isotopically coded, fluorescent, and photocleavable under MALDI-MS conditions. These characteristics facilitate the detection and identification of cross-linked proteins and BiPS-containing peptides (cross-links).

Our study of the RNase S model protein complex demonstrated that fluorescence assists in both the detection of cross-linked proteins in a gel and fluorescent cross-links during the HPLC separation. The isotopic coding facilitates the process of MS detection of the cross-link and its constituent peptides released after cross-linker photocleavage. The benefits of the partial photoinduced cleavage of BiPS in

MALDI-MS experiments are 2-fold. First, the masses and mass differences of the peptides obtained by photocleavage of BiPS are in a defined relation to each other, providing MS signatures for immediate assignment of cross-link types (dead end, intra-, or interpeptide). Second, the identification of cross-links is greatly improved because separate MS/MS analyses of the individual cross-linked peptides can be performed. A software program we developed termed ICC-CLASS uses these MS features for automated detection, assignment, and identification of BiPS cross-links.

The unique advantages of BiPS and the automation capabilities provided by ICC-CLASS facilitate the use of this cross-linking approach for structural studies in biological systems where other structural analysis methods are limited, for example in the study of receptor proteins. In this study, we describe the successful identification of the binding site of a phosphopeptide mimicking the phosphorylated C terminus of

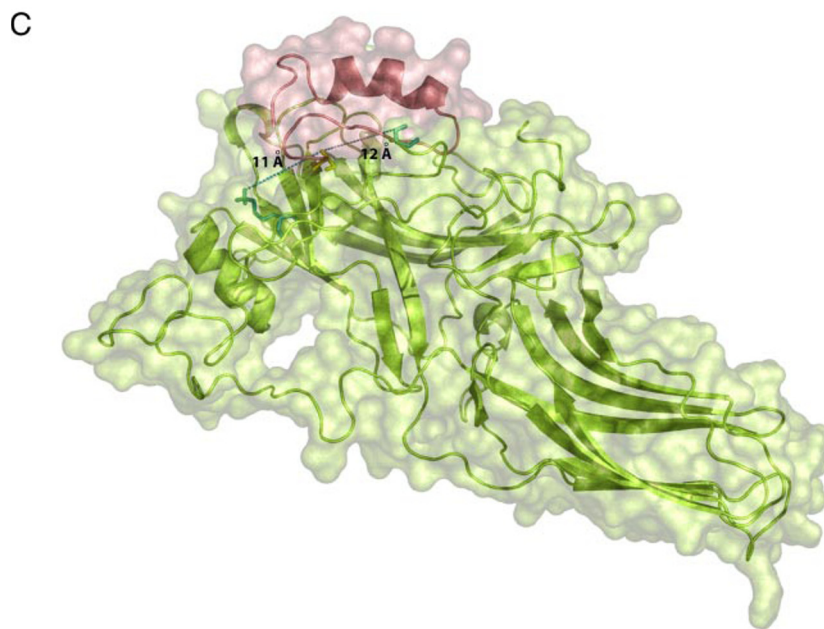
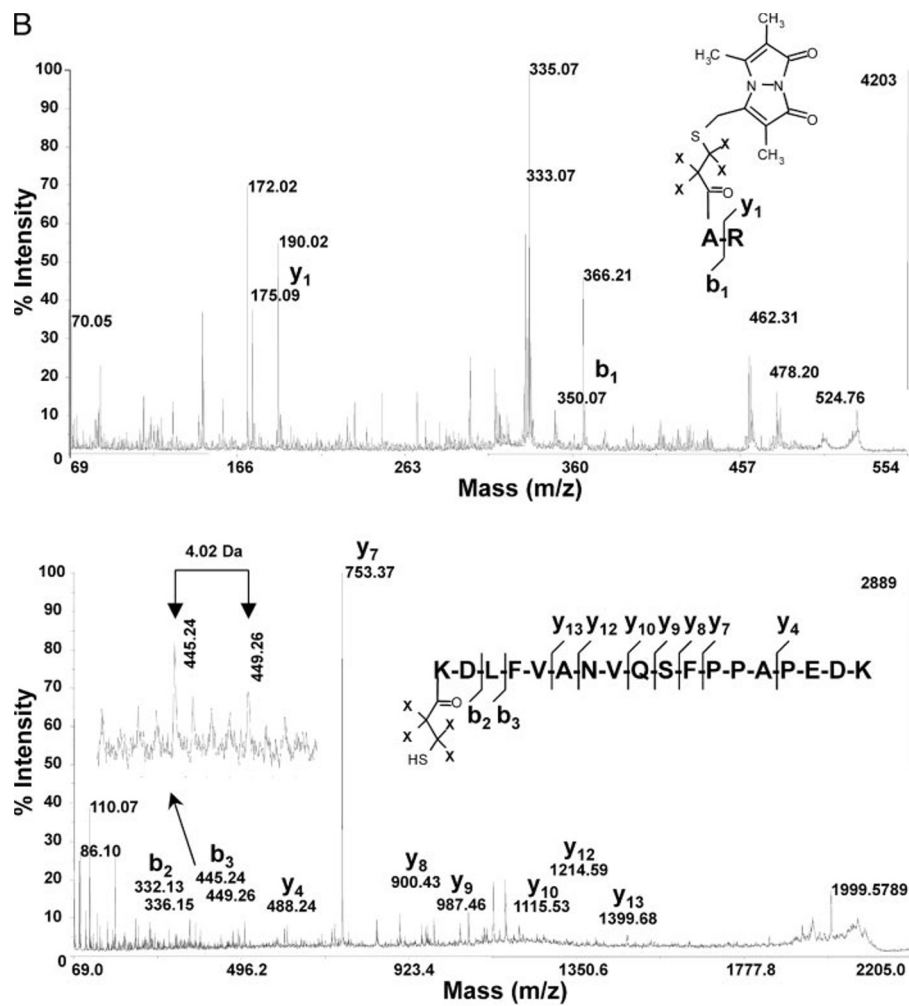


FIG. 3—continued



V<sub>2</sub>R to its adaptor,  $\beta$ -arrestin. This combination of cross-linker and software should be useful for mapping the docking sites of the intact receptor and arrestin or even more complex signaling modules, or signalosomes, either *in vitro* or *in vivo*.

**Acknowledgments**—We are thankful to the University of North Carolina-Duke Proteomics Facility for use of the mass spectrometers and to the anonymous donor for supporting research in proteomics. We gratefully acknowledge Professor Robert J. Lefkowitz (Duke University Medical Center and Howard Hughes Medical Institute, Durham, NC) for useful discussions. We also thank Kelly Nobles for providing the purified  $\beta$ -arrestin protein used in these studies.

\* This work was supported in part by Genome Canada, Genome British Columbia, Muscular Dystrophy Association Grant MDA3720, American Heart Association Grant 0665361U, and North Carolina Biotechnology Center Grant 2006-MRG-1107 (to N. V. D.). The costs of publication of this article were defrayed in part by the payment of page charges. This article must therefore be hereby marked "advertisement" in accordance with 18 U.S.C. Section 1734 solely to indicate this fact.

¶ Supported by an award from the American Heart Association and by a Ruth L. Kirschstein Institutional Award.

|| To whom correspondence should be addressed: Dept. of Biochemistry and Microbiology, University of Victoria-Genome British Columbia Proteomics Centre, University of Victoria, 3101-4464 Markham St., Vancouver Island Technology Park, Victoria, British Columbia V8Z7X8, Canada. Tel.: 250-483-3221; Fax: 250-483-3238; E-mail: christoph@proteincentre.com.

# REFERENCES

1. Sinz, A. (2003) Chemical cross-linking and mass spectrometry for mapping three-dimensional structures of proteins and protein complexes. *J. Mass Spectrom.* **38**, 1225–1237
2. Sinz, A. (2006) Chemical cross-linking and mass spectrometry to map three-dimensional protein structures and protein-protein interactions. *Mass Spectrom. Rev.* **25**, 663–682
3. Back, J. W., De Jong, L., Muijsers, A. O., and De Koster, C. G. (2003) Chemical cross-linking and mass spectrometry for protein structural modeling. *J. Mol. Biol.* **331**, 303–313
4. Sinz, A., and Wang, K. (2001) Mapping protein interfaces with a fluorogenic cross-linker and mass spectrometry: application to nebulin-calmodulin complexes. *Biochemistry* **40**, 7903–7913
5. Young, M. M., Tang, N., Hempel, J. C., Oshiro, C. M., Taylor, E. W., Kuntz, I. D., Gibson, B. W., and Dollinger, G. (2000) High throughput protein fold identification by using experimental constraints derived from intramolecular cross-links and mass spectrometry. *Proc. Natl. Acad. Sci. U. S. A.* **97**, 5802–5806
6. Kruppa, G. H., Schoeniger, J., and Young, M. M. (2003) A top down approach to protein structural studies using chemical cross-linking and Fourier transform mass spectrometry. *Rapid Commun. Mass Spectrom.* **17**, 155–162
7. Muller, D. R., Schindler, P., Wirth, U., Voshol, H., Hoving, S., and Steinmetz, M. O. (2001) Isotope-tagged cross-linking reagents. A new tool in mass spectrometric protein interaction analysis. *Anal. Chem.* **73**, 1927–1934
8. Back, J. W., Notenboom, V., de Koning, L. J., Muijsers, A. O., Sixma, T. K., de Koster, C. G., and de Jong, L. (2002) Identification of cross-linked peptides for protein interaction studies using mass spectrometry and <sup>18</sup>O labeling. *Anal. Chem.* **74**, 4417–4422
9. Petrotchenko, E. V., Olkhovik, V. K., and Borchers, C. H. (2005) Isotopically coded cleavable cross-linker for studying protein-protein interaction and protein complexes. *Mol. Cell. Proteomics* **4**, 1167–1179
10. Petrotchenko, E. V., Pasek, D., Elms, P., Dokholyan, N. V., Meissner, G., and Borchers, C. H. (2006) Combining fluorescence detection and mass spectrometric analysis for comprehensive and quantitative analysis of redox-sensitive cysteines in native membrane proteins. *Anal. Chem.* **78**, 7959–7966
11. Lefkowitz, R. J., Rajagopal, K., and Whalen, E. J. (2006) New roles for  $\beta$ -arrestins in cell signaling: not just for seven-transmembrane receptors. *Mol. Cell* **24**, 643–652
12. Baker, B. R., Query, M. V., Bernstein, S., Safir, S. R., and Subbarow, Y. (1947) A second synthesis of 2-( $\delta$ -carboxybutyl)-thiophane-3,4-dicarboxylic acid. *J. Org. Chem.* **12**, 167–173
13. Kast, J., Parker, C. E., van der Drift, K., Dial, J. M., Milgram, S. L., Wilm, M., Howell, M., and Borchers, C. H. (2003) Matrix-assisted laser desorption/ionization directed nano-electrospray ionization tandem mass spectrometric analysis for protein identification. *Rapid Commun. Mass Spectrom.* **17**, 1825–1834
14. Borchers, C., Peter, J. F., Hall, M. C., Kunkel, T. A., and Tomer, K. B. (2000) Identification of in-gel digested proteins by complementary peptide-mass fingerprinting and tandem mass spectrometry data obtained on an electrospray ionization quadrupole time-of-flight mass spectrometer. *Anal. Chem.* **72**, 1163–1168
15. Parker, C. E., Warren, M. R., Loisele, D., Dicheva, N. N., Scarlett, C. O., and Borchers, C. H. (eds) (2005) *Identification of Components of Protein Complexes*, in *Methods in Molecular Biology* (Patterson, W. C., ed) Vol. 301, pp. 117–151, Humana Press, New Jersey
16. Xiao, K., Shenoy, S. K., Nobles, K., and Lefkowitz, R. J. (2004) Activation-dependent Conformational Changes in  $\beta$ -arrestin 2. *J. Biol. Chem.* **279**, 55744–55753
17. Nobles, K. N., Guan, Z., Xiao, K., Oas, T. G., and Lefkowitz, R. J. (2007) The active conformation of  $\beta$ -arrestin1. Direct evidence for the phosphate sensor in the N-domain and conformational differences in the active states of  $\beta$ -arrestins1 and -2. *J. Biol. Chem.* **282**, 21370–21381
18. Borchers, C., and Tomer, K. B. (1999) Characterization of the noncovalent complex of human immunodeficiency virus glycoprotein 120 with its cellular receptor CD4 by matrix-assisted laser desorption/ionization mass spectrometry. *Biochemistry* **38**, 11734–11740
19. Ding, F., Dokholyan, N. V., and Shakhnovich, E. (2006) Emergence of protein fold families through rational design. *PLoS Comput. Biol.* **2**, e85
20. Yin, S., Ding, F., and Dokholyan, N. V. (2007) Modeling backbone flexibility improves protein stability estimation. *Structure (Lond.)* **15**, 1567–1576
21. Yin, S., Ding, F., and Dokholyan, N. V. (2007) Eris: an automated estimator of protein stability. *Nat. Methods* **4**, 466–467
22. Rost, B., Sander, C., and Schneider, R. (1994) PHD—an automatic mail server for protein secondary structure prediction. *Comput. Appl. Biosci.* **10**, 53–60
23. Sugita, Y., and Okamoto, Y. (1999) Replica-exchange molecular dynamics method for protein folding. *Chem. Phys. Lett.* **314**, 141–151
24. Chen, R., Li, L., and Weng, Z. (2003) RDOCK: refinement of rigid-body protein docking predictions. *Proteins* **52**, 80–87
25. Wiehe, K., Pierce, B., Mintseris, J., Tong, W. W., Anderson, R., Chen, R., and Weng, Z. (2005) ZDOCK and RDOCK performance in CAPRI rounds 3, 4, and 5. *Proteins* **60**, 207–213
26. Kim, E. E., Varadarajan, R., Wyckoff, H. W., and Richards, F. M. (1992) Refinement of the crystal structure of ribonuclease S. Comparison with and between the various ribonuclease A structures. *Biochemistry* **31**, 12304–12314
27. Gurevich, V. V., and Gurevich, E. V. (2006) The structural basis of arrestin-mediated regulation of G-protein-coupled receptors. *Pharmacol. Ther.* **110**, 465–502